A dominant mutation within the DNA-binding domain of the bZIP transcription factor *Maf* causes murine cataract and results in selective alteration in DNA binding

Mary F. Lyon[1,*,†], Robyn V. Jamieson[2,3,†], Rahat Perveen[2], Peter H. Glenister[1], Robert Griffiths[1], Yvonne Boyd[1,4], Laurie H. Glimcher[5], Jack Favor[6], Francis L. Munier[7] and Graeme C. M. Black[2,8]

[1]Mammalian Genetics Unit, Harwell, Didcot, OX11 0RD, UK, [2]Academic Unit of Medical Genetics and Regional Genetics Service Department of Clinical Genetics, Central Manchester and Manchester Children's University Hospitals NHS Trust, St Mary's Hospital, Hathersage Road, Manchester M13 0JH, UK, [3]Department of Clinical Genetics, The Children's Hospital at Westmead, Sydney, Australia, [4]Institute of Animal Health, Compton, Newbury RG20 7NN, UK, [5]Department of Immunology, Harvard School of Public Health, Boston MA 02115-6017, USA, [6]Institute of Human Genetics, GSF-Research Centre for Environment and Health, D-85764 Neuherberg, Germany, [7]Hopital Ophthalmique Jules Gonin, Center Hospitalier Universitaire Vaudois, Lausanne, Switzerland and [8]Academic Unit of Ophthalmology, Manchester Royal Eye Hospital, Oxford Road, Manchester M13 9WH, UK

The murine autosomal dominant cataract mutants created in mutagenesis experiments have proven to be a powerful resource for modelling the biological processes involved in cataractogenesis. We report a mutant which in the heterozygous state exhibits mild pulverulent cataract named 'opaque flecks in lens', symbol *Ofl*. By molecular mapping, followed by a candidate gene approach, the mutant was shown to be allelic with a knockout of the bZIP transcription factor, *Maf*. Homozygotes for *Ofl* and for *Maf* null mutations are similar but a new effect, renal tubular nephritis, was found in *Ofl* homozygotes surviving beyond 4 weeks, which may contribute to early lethality. Sequencing identified the mutation as a G→A change, leading to the amino-acid substitution mutation R291Q in the basic region of the DNA-binding domain. Since mice heterozygous for knockouts of *Maf* show no cataracts, this suggests that the *Ofl* R291Q mutant protein has a dominant effect. We have demonstrated that this mutation results in a selective alteration in DNA binding affinities to target oligonucleotides containing variations in the core CRE and TRE elements. This implies that arginine 291 is important for core element binding and suggests that the mutant protein may exert a differential downstream effect amongst its binding targets. The cataracts seen in *Ofl* heterozygotes and human *MAF* mutations are similar to one another, implying that *Ofl* may be a model of human pulverulent cortical cataract. Furthermore, when bred onto a different genetic background *Ofl* heterozygotes also show anterior segment abnormalities. The *Ofl* mutant therefore provides a valuable model system for the study of *Maf*, and its interacting factors, in normal and abnormal lens and anterior segment development.

INTRODUCTION

Cataract is the commonest preventable cause of blindness worldwide. Inherited autosomal dominant cataract represents around half of congenital forms. Several underlying genes have now been identified, in particular those affecting lens membrane and crystallin genes (1). However in many families the genetic basis remains undefined. Twin studies have recently

---

shown that genetic factors account for approximately 50% of the contribution to age-related cataract (2). While the specific genetic contributors are not known, the genes identified in congenital cataract—particularly those associated with pro-gressive phenotypes—represent attractive candidates.

Mutagenesis experiments in mice have led to the production of a large resource, with ∼200 murine dominant cataract mutants generated (3). Offspring have been scored for cataracts after parental (usually male) mutagenic treatment. Many mutants have been mapped and the molecular basis defined, including mutations in genes for crystallins, the lens protein *Lim2*, the lens-specific gap junction protein *Gja8*, and the transcription factors *Pax2*, and *Pax6*. These provide excellent mammalian models for human cataractogenesis (3).

MAF has been identified as a human disease gene associated with presenile cataract (4). MAF, a bZIP transcription factor, is expressed early in the development of the lens and differentiat-ing lens fibres, and is central to lens crystallin gene regulation (5,6). It functions as both a homo and heterodimer and binds to maf response elements (MAREs) (7,8). Homozygous null mutant *Maf* mouse embryos have defective lens formation, small eyes and decreased expression of crystallins (5,9,10). Heterozygous null mice exhibit normal eye development.

We report a murine form of cataract, designated *Ofl* (opaque flecks in lens), resulting from *Maf* mutation. The R291Q missense mutation substitutes a conserved residue in the DNA-binding domain of Maf. Electromobility shift assays (EMSAs) on the mutant protein demonstrate loss of binding to variant MARE oligonucleotides. Heterozygotes exhibit a cataract similar in phenotype to the heterozygous R288P human *MAF* mutation. When bred onto a different genetic background *Ofl* heterozygotes also show anterior segment abnormalities. The *Ofl* mutant therefore provides a valuable model system in the study of Maf and its interacting factors in normal and abnormal lens and anterior segment development.

RESULTS

Ofl mice

The original mutant animal was found amongst offspring in a mutagenesis experiment at the Institute of Mammalian Genetics, Neuherberg. Males of genotype (C3H/HeEl × 102/El)F_1 were irradiated with a dose of 1.5 Gy X-rays and mated at such an interval afterwards that treated spermatogonial stem cells were sampled (11). The mutant animal, J-361, had an 'opaque flecks in the lens' phenotype, from which was derived the symbol *Ofl*.

When the animal was mated to homozygous wild-type, offspring with a similar pulverulent cataract phenotype were produced (Fig. 1A). To test Mendelian segregation further animals were crossed with strains C3H/HeH and 102/ElH (Table 1).

In the cross with C3H/HeH, there was 1:1 segregation ($\chi^2 = 0.0098$; $P > 0.90$), indicating complete penetrance and normal viability. No marked variation in expression was observed.

Among the offspring of crosses with 102/ElH, there was a shortage of affected animals ($\chi^2 = 7.76$; $P < 0.01$). Some of
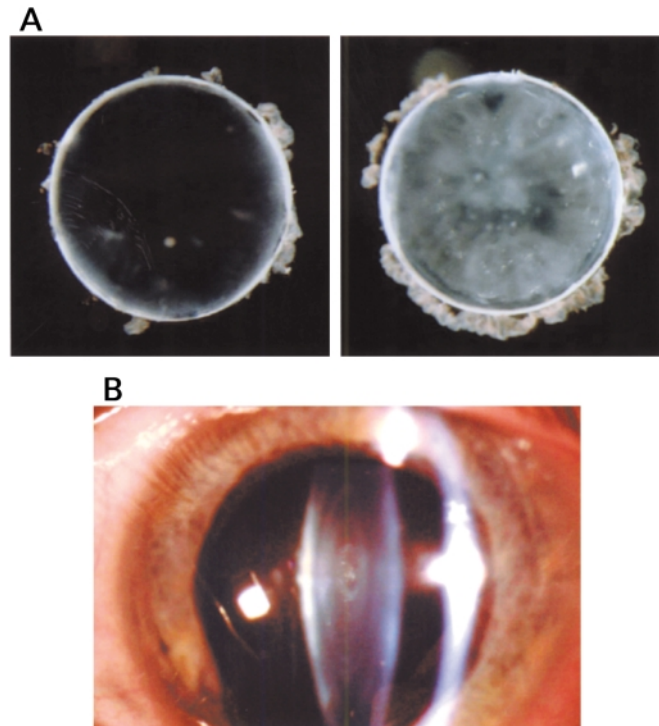

Figure 1. Eye defects in mouse and human *Maf/MAF* heterozygotes. (**A**) Lenses of normal (left) and *Maf*^{Ofl}/+ (right) mice showing pulverulent cataract in *Maf*^{Ofl}/+. (**B**) Eye of human *MAF* heterozygote showing pulverulent catar-act. For a full clinical presentation of the human patients see (4).

Table 1. Results of breeding from *Ofl*/+ heterozygotes

Parents	Offspring			
			Small eyes	
	Cataract	Normal	Unfed	Lived
Ofl/+ × +/+(C3H/HeH)	204	206	—	—
Ofl/+ × +/+(102/ElH)	202[a]	262	—	—
Ofl/+ × *Ofl*/+	205	119	34	15
Maf$^-$/+ × *Ofl*/+	74[b]		1	12

[a]Twenty-five were of atypical appearance.
[b]These mice were not scored for cataract.

those scored as affected had an atypical phenotype. The pupil was only partly dilated and the lens misshapen. Without atropine the pupil was of normal size. Of 202 affected animals 25 (12.4%) were of this type, and of the 19 pairs of parents that produced at least 10 young, 11 produced at least one atypical animal.

Thus, the 102/ElH genetic background appears to affect both penetrance and expressivity of the *Ofl* mutation. Forty mice of strain 102/ElH were examined and no eye abnormalities were detected, excluding the possibility that this atypical cataract was not due to the *Ofl* gene but to a new cataract segregating in the 102/ElH substrain. Two atypical animals crossed with 102/ElH produced both typical and atypical *Ofl* young.

Genetic mapping of *Ofl*

Mapping with visible markers assigned the *Ofl* locus to chromosome(Chr) 8, between the markers *Os* and $Mc1r^{E-so}$ with recombination *Os* $(30.1 \pm 4.7) - Ofl (11.8 \pm 3.4) - Mc1r^{E-so}$ (data not shown). For refined mapping, offspring of an interspecific backcross with *Mus spretus* were scored for cataract and for Chr 8 microsatellite markers. Among 159 offspring the results were *D8Mit242* $(7/159) - D8Mit115$ $(10/159) - Ofl (5/159) - D8Mit55$, giving recombination percentages *D8Mit242* $(4.40 \pm 1.63) - D8Mit115 (6.29 \pm 1.93) - Ofl$ $(3.14 \pm 1.38) - D8Mit55$. The *Ofl* locus was thus placed at position ca. 60 cM on the consensus map, a region which contains the locus of the transcription factor *Maf*.

Preparation of homozygotes

Among intercrosses of *Ofl*/+ × *Ofl*/+ intended to produce animals homozygous for *Ofl*, some females were dissected when 14.5–16.5 days pregnant and others were allowed to go to term. Among the young studied as fetuses there were some with small eyes (Fig. 2D and Table 2). The ratio of normal to small-eyed fetuses showed agreement with the 3:1 ratio expected if the abnormal fetuses were homozygotes ($\chi^2 = 0.25$; $0.5 < P < 0.7$). Sectioning revealed failure of differentiation of the lens fibres, which remained in the state of columnar epithelium (Fig. 2E and F). This was very similar to that described for homozygous *Maf* null fetuses.

Among litters allowed to go to term there were again animals with visibly small eyes, specifically small pupils. Externally they appeared otherwise normal, with a normal colour and level of activity. However, the majority failed to feed and died or disappeared within 24 h. The remainder survived to at least 2 weeks of age, when they appeared small and with a tremor (Fig. 2A). The lenses remained undifferentiated (Fig. 2C). These small animals died at various ages over the following few weeks.

Statistical tests of agreement with an expected 3:1 ratio of normal to small-eyed showed a significant shortage of the presumed homozygotes. There were 49/373 homozygotes (13.4%) giving a test for goodness of fit to a 3:1 segregation ratio of $\chi^2 = 28.0$; $P < 0.001$. Among the animals with normal eyes at birth and later scored for cataract, there was a good fit to a 2:1 ratio of 205 *Ofl*: 119 normal ($\chi^2 = 1.68$; $0.1 < P < 0.2$). A total of 12 *Ofl* mice from these intercrosses were tested for homozygosity by breeding, and all bred as heterozygotes. Thus, there is no evidence that the shortage of homozygotes was the result of misclassification due to overlap with the heterozygous phenotype. The shortage of homozygotes could be explained in part at least by death of those that failed to feed before discovery of the litter.

To test the candidacy of *Maf* as the underlying gene for *Ofl*, two Maf^+/Maf^- heterozygous females were crossed with *Ofl*/+ males, and dissected when 15.5 days pregnant. Out of 23 fetuses, four showed typical small eyes on external inspection (Fig. 2D and Table 2), in good agreement with a 3:1 ratio of normal to affected ($\chi^2 = 0.71$; $0.3 < P < 0.5$). Histological sections of small-eyed fetuses confirmed failure of differentiation of lens fibres as seen in Maf^-/Maf^- and *Ofl*/*Ofl* (Fig. 2G). In addition, some crosses of *Ofl*/+ with Maf^+/Maf^- were allowed to go to term and out of 87 young 13 showed a syndrome similar to that seen in both Maf^-/Maf^- and *Ofl*/*Ofl* homozygotes. This was taken as clear evidence that *Ofl* is allelic with *Maf*.

Extraocular manifestations of *Ofl* homozygotes

The syndrome of small eyes, failure to feed, and small size and tremor at weaning age resembles closely the description of post-natal homozygous *Maf* null animals (5,9,10). In an attempt to find causes for the small size and premature death, three Maf^-/Ofl animals were killed and dissected when 105–117 days old. The post mortem revealed kidneys which were grossly abnormal to the naked eye, pale in colour and with a lumpy surface. Histological sections showed marked tubular nephritis with dilated tubules containing eosinophil casts in some cases (Fig. 2I and J). Other organs appeared histologically normal.

To investigate this abnormality further, urine of *Ofl*/*Ofl* and Maf^-/Ofl mice was tested with reagent strips (Combur Test, Roche Diagnostics, UK), and more histological sections were studied. Urine of affected animals tested positive for glucose from about 4 weeks of age and progressed from 50 mg/100 ml at 4 weeks to 300 or 1000 mg/100 ml at around 7–8 weeks. Tests of blood glucose and plasma insulin levels were in the normal range; hence the urinary abnormality was regarded as of renal origin. Some *Ofl*/*Ofl* animals were killed at ages ranging from 17 to 46 days, and Maf^-/Ofl at 50–57 days. In two mice aged 17 and 20 days no kidney abnormality was observed, but in two mice aged 26 and 30 days patches of dilated tubules were visible. At ages of 46, 50 and 57 days patches of dilated tubules were again visible, some with eosinophil casts. The degree of severity varied among the animals, the kidneys of the 50-day-old mouse being as severely affected as those of the 117-day-old animal. Few animals were available for study because of the early deaths of both *Ofl*/*Ofl* and Maf^-/Ofl, but on the evidence available the abnormalities in the two genotypes were similar.

Ofl/+ phenotype

On first examination of the eyes of *Ofl*/+ at 4–6 weeks of age pulverulent cataracts were present (Fig. 1A). These were similar in appearance to the pulverulent cataracts seen in humans with an R288P MAF mutation (Fig. 1B) and a MAF 16q translocation (4). In *Ofl*/+ mice on a 102/ElH background, in some cases the pupils, which were of normal size without atropine, failed to dilate fully after atropine, suggesting some aberration in development of the anterior segment which was also seen in some human patients with MAF abnormality.

Nature of the *Maf* mutation in *Ofl*

Maf mRNA exists in a single-exon form which encodes a 370 amino acid polypeptide. The coding region was screened for mutation using single-strand conformational polymorphism/heteroduplex analysis on genomic DNA from homozygous, heterozygous and control animals on the C3H/HeE1 and 102/E1 backgrounds. Band abnormality was detected in homozygotes and heterozygotes in a fragment coding for part of the DNA-binding region. Sequencing revealed a G to A transition at
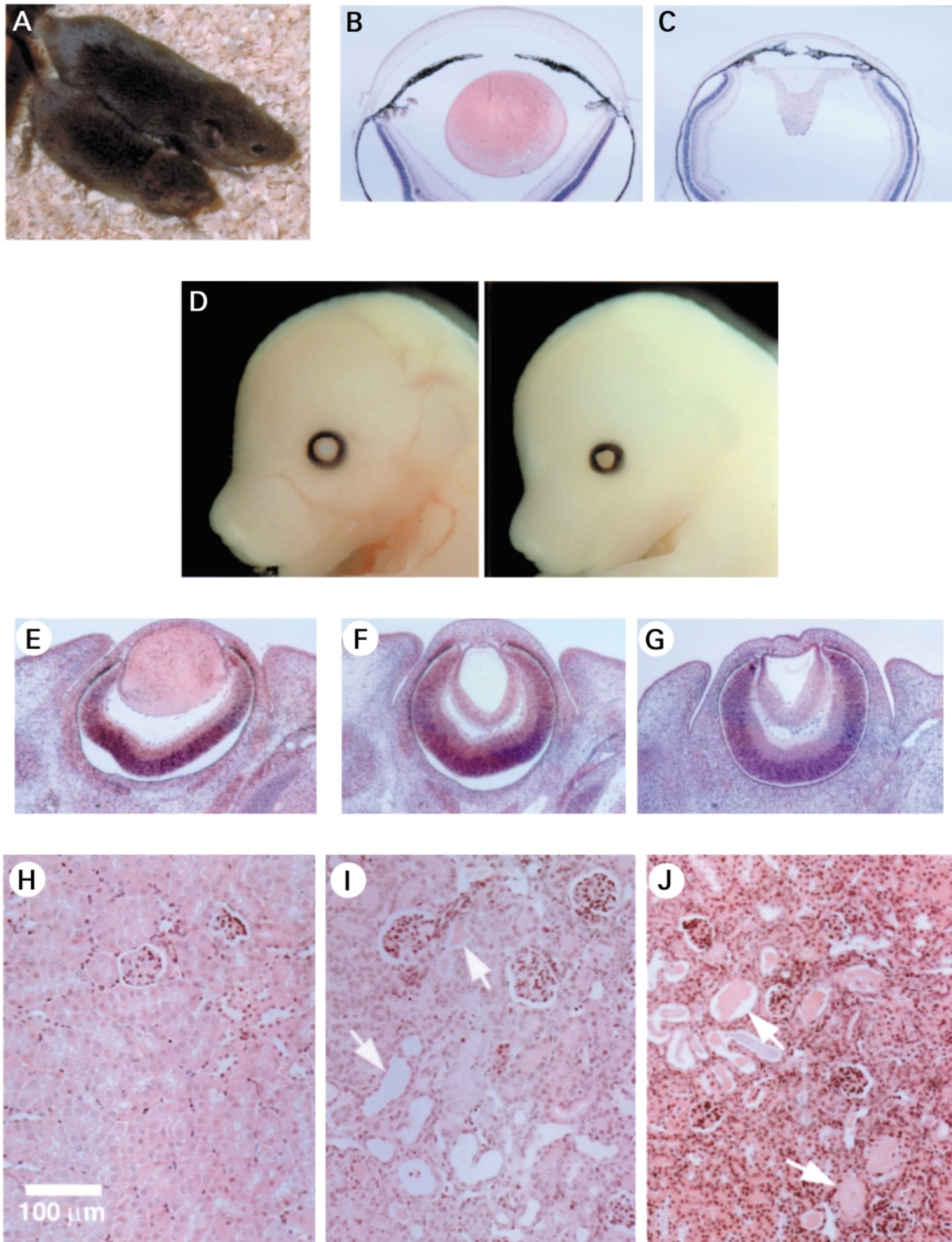
Figure 2. Phenotypes of *Maf*^{Ofl} homozygotes and *Maf*$^{-}$/*Maf*^{Ofl} double heterozygotes. (**A**) *Maf*^{Ofl}/*Maf*^{Ofl} mouse with normal sib aged one month, showing small size and closd eyes. (**B** and **C**) Sections of eyes of *Maf*^{Ofl}/+ or +/+ (B) and *Maf*^{Ofl}/*Maf*^{Ofl} (C) showing rudimentary lens in C. (**D**) Heads of normal (left) and *Maf*$^{-}$/*Maf*^{Ofl} fetuses aged 15.5 days showing visibly small eye in *Maf*$^{-}$/*Maf*^{Ofl}. (**E–G**) Eyes of 15.5 day fetuses showing failure of lens differentiation (E) Normal; (F) *Maf*^{Ofl}/*Maf*^{Ofl}; (G) *Maf*$^{-}$/*Maf*^{Ofl}. (**H–J**) Kidneys of *Maf*^{Ofl}/+ aged 73 days with normal kidney (H), *Maf*^{Ofl}/*Maf*^{Ofl} aged 46 days (I) and *Maf*$^{-}$/*Maf*^{Ofl} aged 50 days (J). (I) and (J) both show dilated tubules, some with eosinophil casts (arrows).
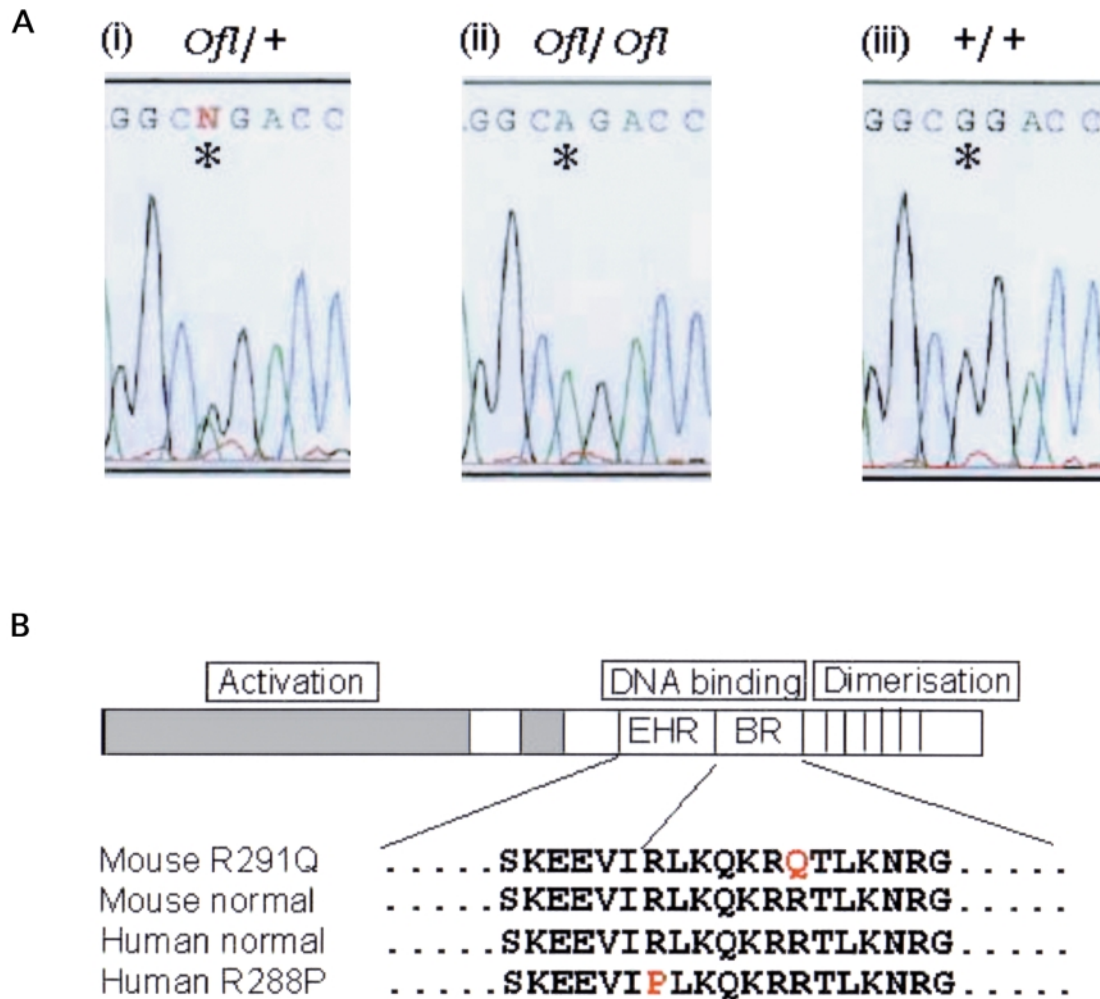
Figure 3. *Maf* sequence in *Ofl*/+ and *Ofl*/*Ofl* mice and location of *Maf*/*MAF* mutations in the DNA-binding domain of the protein. (**A**) Direct sequencing of PCR product from *Ofl*/+, *Ofl*/*Ofl* and control mice. (i) *Ofl*/+, heterozygous mutation, a G to A transition at nucleotide 1803 of *Maf* mRNA (GenBank accession no. S74567), which results in an arginine to glutamine substitution at amino acid 291 of the protein product. (ii) *Ofl*/*Ofl*, homozygous mutation at nucleotide 1803. (iii) Control sequence. (**B**) The DNA-binding domain of MAF contains an extended homology region (EHR) and a basic region (BR). There is strong amino acid sequence conservation in the DNA-binding domain amongst the large Maf proteins and across species (4). Arginine 291 of the mouse Maf protein is conserved in all known large Maf proteins and lies six residues C terminal to the mutated arginine in the R288P human MAF mutation family when the conserved regions are compared. (In all cases an asterisk indicates the position of the mutation.)

Table 2. Dissections of pregnant females

Parents	Number of females	Total implantation	Normal	Small eyes	Moles	Other
Ofl/+ × *Ofl*/+	14	133	78	29	22	4
Maf⁻/+ × *Ofl*/+	2	24	19	4	—	1

Moles = remains of fetuses dying soon after implantation.
Other = four dead at ca. 10 days, one doubtful for small eyes.

nucleotide position 1803 of *Maf* (GenBank accession no. S74567; Fig. 3A). This mutation substitutes an invariant arginine to glutamine at amino acid position 291 (R291Q) in the basic region DNA-binding domain of *Maf* (Fig. 3B). This change was not present in the C3H/HeEl nor 102/El control lines. There was no further *Maf* coding sequence abnormality.

Electromobility shift assays (EMSAs)

EMSAs have been used previously to demonstrate that the MAF protein forms DNA–protein complexes with consensus and variant TRE and CRE like MAREs (7). The TNT Coupled Wheat Germ Extract System (Promega) was used in transcription/translation reactions to generate peptides containing the DNA-binding and leucine zipper domains of the R291Q mutant and control proteins. Translation products were analysed after labelling with [³⁵S]methionine (Fig. 4A). EMSAs revealed binding of the wild-type peptide to various oligonucleotides as previously reported (Figs 4B and 5 and Table 3). Specificity of binding was demonstrated by the addition of the unlabelled
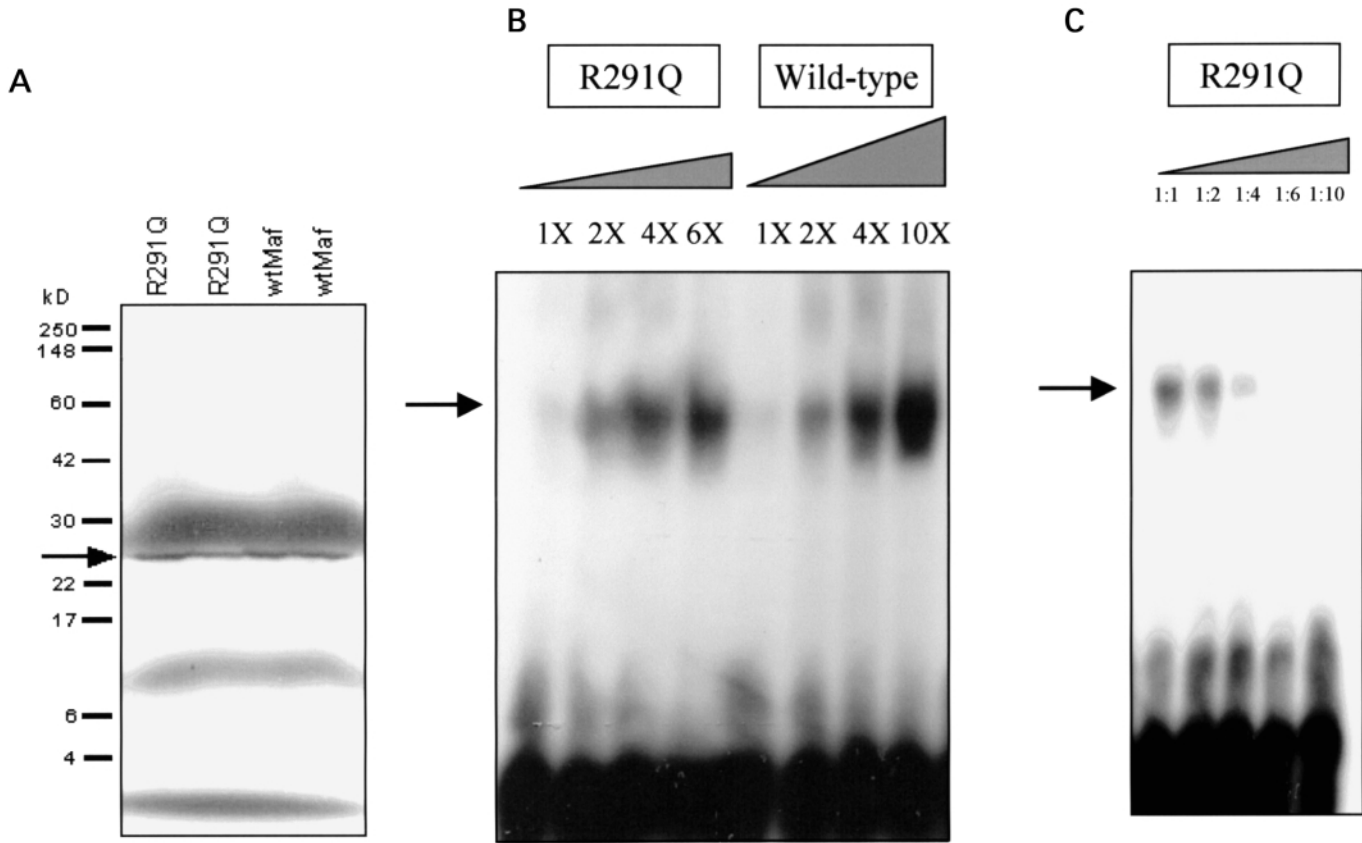
Figure 4. (**A**) *In vitro* translation of Maf protein and control EMSAs. R291Q mutant and wild-type *Maf* were translated *in vitro* in the presence of [35S]methionine and analysed by SDS gel electrophoresis. Bands at 30, ~10 and ~2 kDa represent background from wheat germ extract. Arrow shows translated Maf polypeptide. (**B**) Concentration-dependent binding of Maf proteins. An increasing amount of mutant (left) and wild-type (right) Maf was added to the labelled MARE oligonucleotide (oligo 4) to demonstrate concentration-dependent binding. The protein–oligonucleotide complexes are arrowed. (**C**) Concentration-dependent competition of R291Q mutation with wild-type MAF for DNA binding. A reduction in the binding of the wild-type protein to oligonucleotide 1 in the presence of increasing amounts of R291Q mutant MAF protein is demonstrated. The protein–oligonucleotide complexes are arrowed.

Table 3. Oligonucleotide sequences and binding to mutant and wild-type Maf proteins

Oligonucleotide[a]	Sequence[b]	Binding	
		Maf control	Maf R291Q
1 (1)	TGCTGACTCAGCA	+	+
2 (2)	TGCTGACGTCAGCA	+	+
3 (3)	TGCTGATTCAGCA	+	−
4 (9)	TGCCGACTCGGCA	+	−
5 (28)	TGCCGACGTCATCC	+	−
6 (30)	TGCCGACGTCATTG	+	−

[a]Bracketed number refers to previously assigned oligonucleotide number (7).
[b]Nucleotide sequences of only the varied consensus elements of the oligonucleotides are shown. Nucleotides matches with the MAREs are underlined.

oligonucleotide in each case, which successfully competed and abolished the visible MAF–MARE complex, whereas unlabelled non-specific competitor did not (Fig. 5). The mutant, with glutamine substituted for arginine (R291Q), showed variability in binding with absence of binding with 4/6 oligonucleotides tested (oligonucleotides 3, 4, 5 and 6; Fig. 5 and Table 3) compared with the normal protein. The MAF

proteins showed concentration-dependent binding to the oligonucleotides (Fig. 4B); Furthermore, for the oligonucleotides to which it bound, the mutant Maf protein demonstrated competition with the wild-type protein (Fig. 4C). The 13 bp TRE-type MARE contains the *cis* element TRE (TGACTCA), while the 14 bp CRE-type MARE contains the CRE element (TGACGTCA) in the middle. Absence of binding with the R291Q mutant was seen when there was variation in these core binding sequences with or without the presence of variation in the 3 bp extended elements either side. The R291Q mutation impairs DNA-binding with certain MARE-like oligonucleotides and the R291 residue may be particularly important for core binding.

DISCUSSION

This work provides evidence that the *Ofl/+* pulverulent cataract mutant involves a mutation in the *Maf* transcription factor. Mapping studies demonstrate that the *Ofl* locus lies close to that of *Maf*. The eye defects in *Ofl/Ofl* homozygotes strongly resemble those in *Maf* null homozygotes and *Ofl/+* × *Maf⁻/+* crosses produced young with a similar phenotype, indicating non-complementation. Mutation analysis revealed an
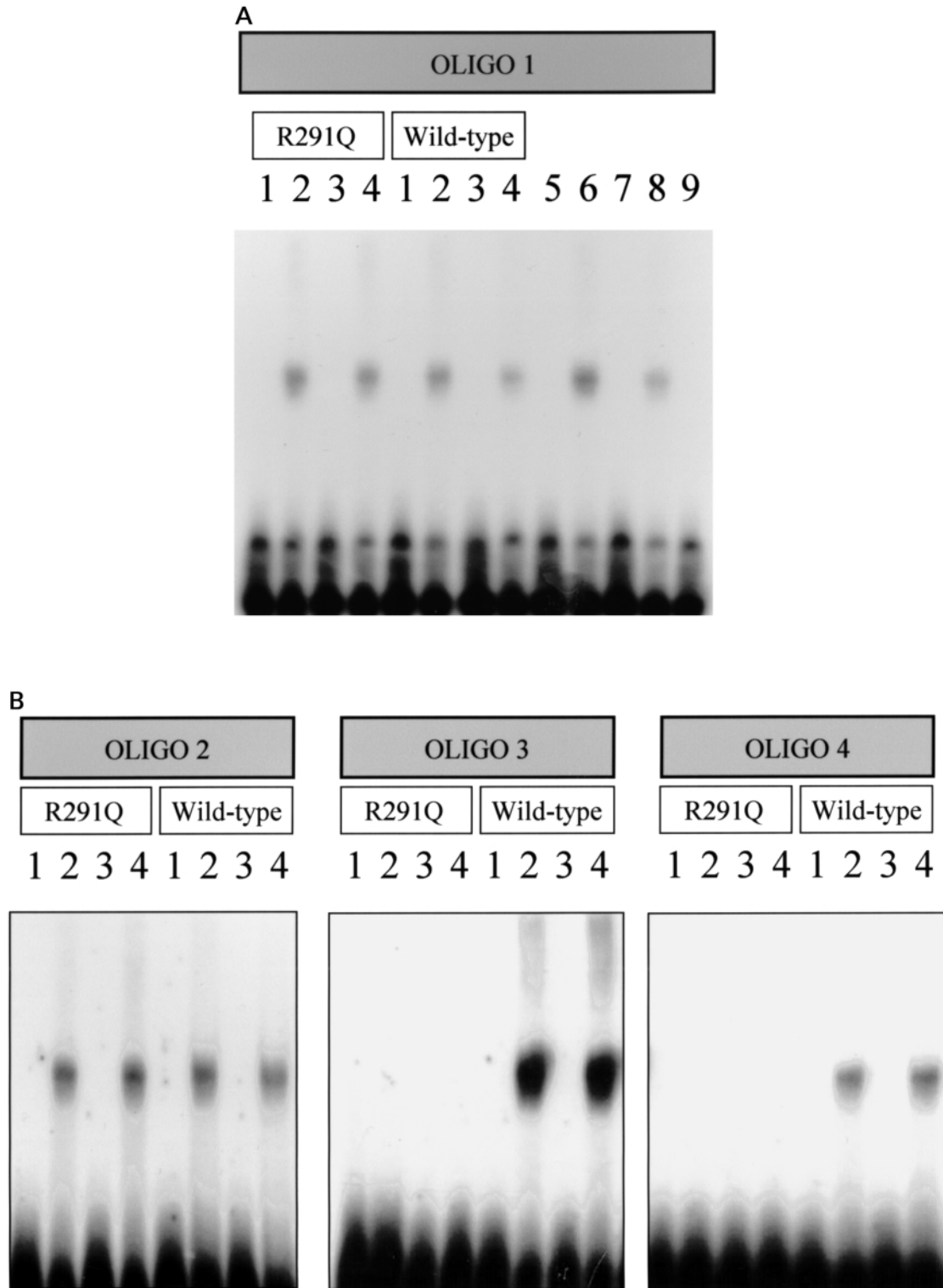
Figure 5. (**A**) DNA-binding activity of *in vitro* translated R291Q mutant and wtMaf to MARE oligonucleotide 1 (see Table 3). Both the mutant and wild-type Maf proteins bind to the consensus TRE core element. Immunoprecipitation to remove the translated, FLAG-tagged protein using ANTI-FLAG® M2 Affinity Gel reduced DNA binding [lanes 5 (R291Q) and 7 (wild-type Maf)]. The recovered, immunoprecipitated protein demonstrated normal DNA binding [lanes 6 (R291Q) and 8 (wild-type Maf)]. *In vitro* translation of a control luciferase template (lane 9) demonstrated no DNA binding. (**B**) DNA-binding activity of *in vitro* translated R291Q mutant and wild-type Maf to further MARE oligonucleotides. Both the mutant and wild-type Maf proteins bind to the consensus element with a CRE core (oligo 2) while variation in the core sequence (oligos 3 and 4) demonstrate loss of binding by the R291Q mutant protein but not the wild-type Maf protein. Lane 1, negative control; lane 2, Maf protein; lane 3, additional specific competitor oligonucleotide; lane 4, additional non-specific competitor.

R291Q substitution in the DNA-binding domain of the Maf protein which is present in heterozygous form in *Ofl/+*, homozygous in *Ofl/Ofl* and absent in the parent line that underwent mutagenesis. In view of the clear evidence that *Ofl* involves a mutation in the *Maf* gene, the symbol should be changed to Maf^{Ofl}.

MAF gene involvement has been identified in two human cataract families both with pulverulent cataract, one with a translocation and the other with an R288P substitution in the basic region of the DNA-binding domain close to the R291Q mouse mutation (4). Maf^{Ofl} also results in pulverulent cataract, providing a valuable model of mammalian cataract.

In homozygotes for Maf^{Ofl} and for the null alleles there are additional non-ocular manifestations. The proportions of Maf^{Ofl}/Maf^{Ofl} and Maf^{-}/Maf^{Ofl} were normal at 14.5–16.5 days gestation. However, fewer than expected Maf^{Ofl}/Maf^{Ofl} homozygotes were found at birth and, while externally normal, the majority failed to feed and died. This has been reported for the null alleles, and was also seen with Maf^{-}/Maf^{Ofl} animals. Kim *et al.* (9) reported death of null homozygotes at 17.5–18.5 days gestation, but this has not been studied in Maf^{Ofl}/Maf^{Ofl}. Maf^{Ofl}/Maf^{Ofl} and Maf^{-}/Maf^{Ofl} animals that fed and survived to 2 weeks of age were small in size [also reported by Kim *et al* (9) in *Maf* null homozygotes] and showed significant tremor. With the other two knockouts, almost no homozygotes survived to weaning age, suggesting that Maf^{Ofl}/Maf^{Ofl} and Maf^{-}/Maf^{Ofl} animals were less severely affected than the homozygous null animals. However, there was some variation reported among the three knockouts and it is not clear whether this apparently poorer survival of the null homozygotes is a real effect, or depends on genetic background or environmental conditions. Among Maf^{Ofl}/Maf^{Ofl} and Maf^{-}/Maf^{Ofl} homozygotes that survived beyond one month a new effect, of tubular nephritis, was found. The mechanism by which *Maf* mutation produces the nephritis, the small size and the shaky behaviour is not known although it is of note that *Maf* is expressed in kidney and brain (5).

The R291Q substitution occurs in a conserved arginine residue, the seventh in the basic region of the highly-conserved DNA-binding domain of large Maf proteins (Fig. 3). It replaces a basic positively charged polar residue with an electrically neutral glutamine. Structural motif comparisons show that this residue is the last amino acid of a sequence that resembles a helix–turn–helix DNA-binding motif that may make direct DNA contacts (12).

EMSA analysis of the R291Q protein reveals loss of DNA-binding activity with a subset of MARE-like oligonucleotides, confirming that R291 is a critical residue for DNA-binding. Loss of binding (with oligonucleotide 4 in our study) had previously been demonstrated when this residue was artificially substituted with glutamate (7). DNA-binding of R291Q with two MARE-like oligonucleotides was indistinguishable from normal on gel shift assay. The 13 and 14 bp consensus binding sequences of the MAREs contain core TRE and CRE elements with extended recognition elements on both sides (7). *In vitro* analysis reveals that none of the residues in the MAREs are completely conserved (7) and lack of conservation is also a feature of potential MAREs recognized in the promoters of a variety of crystallin genes (10). Loss of binding was observed when the core TRE or CRE element contained a mismatch with or without extended element conservation (oligonucleotides 3, 4, 5 and 6). This implies that arginine 291 is critical for core element binding and suggests that the mutant protein is likely to exert a differential downstream effect amongst its binding targets.

Comparison of lens phenotypes for *Maf* mutation suggests that the Maf^{Ofl} substitution mutation is dominant-negative in its effect. The eye phenotype in homozygotes for the three *Maf* knockouts closely resembles that in Maf^{Ofl}/Maf^{Ofl} homozygotes. The lens vesicle forms normally and separates from the overlying future cornea. The anterior lens epithelium appears normal but lens fibre cells fail to differentiate and remain as columnar epithelium. Heterozygotes for each of the three null alleles reveal no specific ocular anomalies. This is in contrast to the Maf^{Ofl} heterozygote ($Maf^{Ofl}/+$), which demonstrates a juvenile pulverulent cataract. This shows that, as well as being important in lens fibre differentiation, Maf is required for maintaining lens fibre clarity. Maf functions as a dimer and is able to form homo- and heterodimers (13,14). In the heterozygous form it is likely that the R291Q allele interferes in a dominant-negative, or dominant-dysregulatory, manner with dimer function since a phenotypic effect is seen, i.e. cataract is present compared with the absence of a phenotype where haploinsufficiency is present. This is similar to the variability in phenotypes seen with dominant-negative and haploinsufficiency mutations in *Mitf*, a basic helix–loop–helix–leucine–zipper transcription factor which also functions as a dimer (15).

It is recognized that marked genetic heterogeneity exists amongst the causes of anterior segment and lens abnormalities. Modifier effects with different strains have been observed in other mouse anterior segment mutants (16,17). It is likely that the phenotypic heterogeneity present in humans in these conditions, including the MAF phenotype, is also contributed to by different alleles of critical interacting genes. Anterior segment abnormality (e.g. iris coloboma, microcornea, Peters anomaly) was present in some of the human patients with the MAF R288P mutation and MAF translocation. When mouse Maf^{Ofl} was crossed with C3H/HeH the heterozygous mutant showed good penetrance and constant expressivity, with pulverulent cataract and no other anomalies. However, when crossed with 102/ElH there was a shortage of affected animals, suggesting incomplete penetrance while the appearance of a new phenotype, with irregularities of the pupil and lens, suggests that genetic modifiers contributed to the ocular abnormalities produced by the Maf^{Ofl} mutation. This points to the importance of *Maf* interacting factors in development of the anterior segment and suggests that the *Ofl* mutant is a valuable model for the study of the genetic factors underlying normal and abnormal lens and anterior segment development.

MATERIALS AND METHODS

Mouse breeding

The mice described here were bred at Harwell in accordance with guidelines issued by the Medical Research Council in

'Responsibility in the use of animals for medical research' (July 1993) and under Home Office project licences 30/000875 and 30/1517. The stock was maintained by crossing *Ofl*/+ mice either to inbred strain C3H/HeH or to strain 102/ElH.

Preliminary mapping was carried out by crosses with visible marker genes. For more detailed mapping *Ofl*/+ female mice were crossed with *Mus spretus* males and *Ofl*/+ offspring were crossed to C3H/HeH to generate an interspecific backcross. Offspring of this backcross were scored for cataract and for polymorphisms of microsatellite markers located in the region of interest indicated by the preliminary mapping, using DNA prepared from the spleen.

The *Maf* knockout heterozygotes were provided by Dr L. Glimcher.

Scoring for cataracts

Scoring for cataracts was carried out at the age of 4–6 weeks. Dilation of the pupil was achieved with a drop of 1% atropine sulfate (Schering-Plough Ltd, UK) applied at least 10 min before examination. Eyes were examined at $20\times$ magnification using a slit-lamp (Zeiss 30SL/M).

Histology

For fetuses and newborn animals whole heads were sectioned whereas for older animals whole eyes were used. Material from fetuses was fixed in Bouin's fixative or 10% neutral formal-saline and post-natal samples were fixed in formal-saline. Samples were embedded in paraffin wax, sectioned and stained with haematoxylin and eosin. For kidney histology material was fixed in formal-saline.

Mutation analysis

Genomic DNA was extracted from murine *Ofl* heterozygotes, homozygotes and control strains C3H/HeH and 102/ElH. PCR amplification of the *Maf* gene was performed (primers on request). DNA (40 ng) was suspended in a 20 µl reaction containing 10 pmol of each forward and reverse primer, 0.75 mM dATP, dGTP, dCTP, dTTP, 67 mM Tris–HCl (pH 8.0), 3.7 mM $MgCl_2$, 6.7 µM EDTA, 16 mM $(NH_4)_2SO_4$ 0.085 mg/ml BSA and 0.1 units of *Taq* DNA polymerase. Owing to the GC sequence content of this gene, some reactions required the addition of enhancing agents either DMSO at 10% or both DMSO at 10% and Betaine at 1 M final concentration. Samples were processed through 30 cycles of amplification consisting of 45 s at 94°C (denaturation), 45 s at 58°C (annealing) and 1 min at 72°C (extension). The final step was lengthened to 10 min. For SSCP/heteroduplex analysis, 1 vol of PCR product was mixed with 1 vol of formamide loading dye and denatured at 96°C for 5 min prior to loading on a 8% acrylamide/bis-acrylamide gel. Gels were run at 350 V overnight at 4°C and silver stained according to standard protocols. Gels were inspected for abnormal bands. Direct sequencing of PCR products were performed using the BigDye™ Terminator Cycle Sequencing Ready Reaction Kit (Applied Biosystems) on a fluorescent sequencer (ABI 377) in accordance to the manufacturer's instructions.

Maf R291Q and control protein expression

On attempting to clone the *Maf* gene we found toxicity to bacterial cells as reported by others (18). In an alternative approach, primers were designed spanning the mutated DNA sequence of interest including regions coding for the DNA-binding domain and the leucine zipper. A T7 promoter/FLAG tagged linker was attached to the forward primer for use of the PCR product in subsequent downstream coupled transcription/translation reactions. Primer pair sequences were as follows: 5'-GGA TCC TAA TAC GAC TCA CTA TAG GAA CAG ACC ACC ATG GAT TAC AAG GAT GAC GAC GAC CGC TTC TCG GAC GAG CAG TTG-3' and 5'-GCG AGC TTG GCC CTG CAA CTA GCA AG-3'. PCR amplification was performed from murine homozygous *Ofl*/*Ofl* and wild-type DNA using the ReddyMix Hi-Fidelity Extensor Master Mix 1 PCR system (Abgene). Transcription/translation reactions were performed using the TNT Coupled Wheat Germ Extract System (Promega) in accordance with the manufacturer's guidelines. Typically 1 µg of template was used in reactions and radiolabelled with [^{35}S]methionine. Reactions were incubated for up to 120 min at 30°C. Translation reactions were analysed using a 4% stacking polyacrylamide gel and a 12% separating gel run in Tris–glycine running buffer. A 5 µl aliquot of the translation reaction was removed and mixed with 20 µl of SDS sample buffer, heated at 100°C for 10 min prior to loading the entire volume initially into the stacking gel alongside a suitable marker (Invitrogen). Samples were subject to electrophoresis through the stacking gel using a constant current of 15 and 30 mA in the separating gel. Gels were run for 3 h and then fixed in fixing solution (50% methanol, 10% glacial acetic acid) for 30 min and further fixed for a further 5 min in 7% acetic acid, 7% methanol and 1% glycerol to prevent the gel from cracking during drying. Gels were dried for 90 min using a conventional gel dryer and exposed overnight at −70°C using Hyperfilm X-ray film.

Immunoprecipitation of FLAG-tagged proteins

FLAG-tagged fusion proteins were immunoprecipitated prior to use in subsequent downstream EMSAs. Immunoprecipitations were performed using the Ezview™Red ANTI-FLAG M2 Affinity Gel in accordance with the manufacturer's guidelines (Sigma). Elution of the FLAG-fusion protein was performed under native conditions by competition with the $3\times$ FLAG peptide in accordance to the manufacturer's guidelines (Sigma). For long-term storage eluted proteins were stored at −20°C.

EMSAs

Transcription/translation products of comparable concentration were used in EMSAs with [^{32}P]labelled double-stranded oligonucleotides. These included the consensus TRE-type MARE (TGCTGACTCAGCA), the consensus CRE-type MARE (TGCTGACGTCAGCA), as well as others with various mismatches in their binding sequences (Table 3) as described previously (7). Gel shift assays were performed using the Gel Shift Assay System (Promega) in accordance with the manufacturer's instructions. The proteins were preincubated at 30°C for 10 min in $1\times$ Gel Shift Binding Buffer (Promega). For

each oligonucleotide positive, negative, specific competitor and random competitor reactions were set up. Competed reactions were carried out using 100 pmol of the same, unlabelled cold oligonucleotide. Non-specific competitor reactions were performed using 0.5 μg/μl of PUC18 DNA. Following incubation 1 μl of ^{32}P was added to each reaction. Incubation was continued for a further 20 min at 30°C. To each reaction 1 μl of 10 × gel loading buffer (250 mM Tris–HCl pH 7.5, 0.2% bromophenol blue, 40% glycerol) was added per reaction and products were analysed on a pre-run 4% polyacrylamide gel in 0.5× TBE (filter-sterilized) for 10 min at 350 V. After loading the samples, gels were run in 0.5× TBE at room temperature at 350 V until the bromophenol blue dye had run three-quarters of the way down the gel, ~45 min. Gels were transferred to a sheet of Whatman 3 MM paper, covered with plastic wrap and dried using a conventional gel dryer at 70°C for 120 min. Gels were exposed to X-ray film 1 h to overnight at −70°C with an intensifying screen. Autoradiograms were then inspected for presence or absence of protein/oligonucleotide binding.

REFERENCES

1. Francis, P.J., Berry, V., Moore, A.T. and Bhattacharya, S. (1999) Lens biology: development and human cataractogenesis. *Trends Genet.*, **15**, 191–196.
2. Hammond, C.J., Duncan, D.D., Snieder, H., de Lange, M., West, S.K., Spector, T.D. and Gilbert, C.E. (2001) The heritability of age-related cortical cataract: the twin eye study. *Invest. Ophthal. Visual Sci.*, **42**, 601–605.
3. Favor, J. and Neuhauser-Klaus, A. (2000) Saturation mutagenesis for dominant eye morphological defects in the mouse *Mus musculus*. *Mamm. Genome*, **11**, 520–525.
4. Jamieson, R.V., Perveen, R., Kerr, B., Carette, M., Yardley, J., Heon, E., Wirth, M.G., van Heyningen, V., Donnai, D., Munier, F. *et al.* (2002) Domain disruption and mutation of the bZIP transcription factor, MAF, associated with cataract, ocular anterior segment dysgenesis and coloboma. *Hum. Mol. Genet.*, **11**, 33–42.
5. Kawauchi, S., Takahashi, S., Nakajima, O., Ogino, H., Morita, M., Nishizawa, M., Yasuda, K. and Yamamoto, M. (1999) Regulation of lens fiber cell differentiation by transcription factor c-Maf. *J. Biol. Chem.*, **274**, 19254–19260.
6. Ogino, H. and Yasuda, K. (2000) Sequential activation of transcription factors in lens induction. *Dev. Growth Differ.*, **42**, 437–448.
7. Kataoka, K., Noda, M. and Nishizawa, M. (1994) Maf nuclear oncoprotein recognizes sequences related to an AP-1 site and forms heterodimers with both Fos and Jun. *Mol. Cell Biol.*, **14**, 700–712.
8. Kerppola, T.K. and Curran, T. (1994) A conserved region adjacent to the basic domain is required for recognition of an extended DNA binding site by Maf/Nrl family proteins. *Oncogene*, **9**, 3149–3158.
9. Kim, J.I., Li, T., Ho, I.C., Grusby, M.J. and Glimcher, L.H. (1999) Requirement for the c-Maf transcription factor in crystallin gene regulation and lens development. *Proc. Natl Acad. Sci. USA*, **96**, 3781–3785.
10. Ring, B.Z., Cordes, S.P., Overbeek, P.A. and Barsh, G.S. (2000) Regulation of mouse lens fiber cell development and differentiation by the Maf gene. *Development*, **127**, 307–317.
11. Favor, J. (1989) Mammalian germ cell mutagenesis data and human genetic risk. *Biol. Zent. bl*, **108**, 309–321.
12. Dlakic, M., Grinberg, A.V., Leonard, D.A. and Kerppola, T.K. (2001) DNA sequence-dependent folding determines the divergence in binding specificities between Maf and other bZIP proteins. *Embo J.*, **20**, 828–840.
13. Kataoka, K., Noda, M. and Nishizawa, M. (1996) Transactivation activity of Maf nuclear oncoprotein is modulated by Jun, Fos and small Maf proteins. *Oncogene*, **12**, 53–62.
14. Kerppola, T.K. and Curran, T. (1994) Maf and Nrl can bind to AP-1 sites and form heterodimers with Fos and Jun. *Oncogene*, **9**, 675–684.
15. Steingrimsson, E., Moore, K.J., Lamoreux, M.L., Ferre-D'Amare, A.R., Burley, S.K., Zimring, D.C., Skow, L.C., Hodgkinson, C.A., Arnheiter, H., Copeland, N.G. *et al.* (1994) Molecular basis of mouse microphthalmia (mi) mutations helps explain their developmental and phenotypic consequences. *Nat. Genet.*, **8**, 256–263.
16. Gould, D.B. and John, S.W. (2002) Anterior segment dysgenesis and the developmental glaucomas are complex traits. *Hum. Mol. Genet.*, **11**, 1185–1193.
17. Smith, R.S., Zabaleta, A., Kume, T., Savinova, O.V., Kidson, S.H., Martin, J.E., Nishimura, D.Y., Alward, W.L., Hogan, B.L. and John, S.W. (2000) Haploinsufficiency of the transcription factors FOXC1 and FOXC2 results in aberrant ocular development. *Hum. Mol. Genet.*, **9**, 1021–1032.
18. Kataoka, K., Nishizawa, M. and Kawai, S. (1993) Structure-function analysis of the maf oncogene product, a member of the b-Zip protein family. *J. Virol.*, **67**, 2133–2141.